

Selective Targeting of AF9 YEATS Domain by Cyclopeptide Inhibitors with Preorganized Conformation

Yixiang Jiang,^{||} Guochao Chen,^{||} Xiao-Meng Li,^{||} Sha Liu, Gaofei Tian, Yuanyuan Li,^{*} Xin Li,^{*} Haitao Li,^{*} and Xiang David Li^{*}Cite This: <https://dx.doi.org/10.1021/jacs.0c10324>

Read Online

ACCESS |



Metrics & More

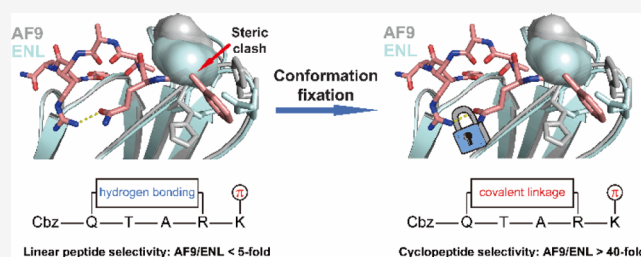


Article Recommendations



Supporting Information

ABSTRACT: YEATS domains are newly identified epigenetic “readers” of histone lysine acetylation (Kac) and crotonylation (Kcr). The malfunction of YEATS–Kac/Kcr interactions has been found to be involved in the pathogenesis of human diseases, such as cancer. These discoveries suggest that the YEATS domains are promising novel drug targets. We and others recently reported the development of YEATS domain inhibitors. Although these inhibitors have a general preference toward the AF9 and ENL YEATS domains, selective inhibitors targeting either YEATS domain are challenging to develop as these two proteins share a high structural similarity. In this study, we identified a proximal site outside the acyllysine-binding pocket that can differentiate AF9 YEATS from ENL YEATS. Combinatorial targeting of both the acyllysine pocket and this additional site by conformationally preorganized cyclopeptides enabled the selective inhibition of the AF9 YEATS domain. The most selective inhibitor, JYX-3, showed a 38-fold higher binding affinity toward AF9 YEATS over ENL YEATS. Further investigations indicated that JYX-3 could engage with AF9 in living cells, disrupt the YEATS-dependent chromatin recruitment of AF9, and suppress the transcription of AF9 target genes.



INTRODUCTION

Chemical inhibitors are valuable tools to probe the biological functions of target proteins. Target selectivity is a key issue when developing a chemical inhibitor. This is especially true when the target protein shares high structural homology with other family members, such as protein kinase.^{1,2} Canonical kinase inhibitors that target structurally conserved adenosine triphosphate (ATP)-binding pockets frequently lead to polypharmacology because of poor selectivity.^{3–10} One strategy to improve the selectivity of a kinase inhibitor involves combinatorial targeting of the ATP pocket and a second site that is more structurally diverse, for example, cavities proximal to the ATP cleft, the substrate-binding region, or regulatory domains of the catalytic pocket.^{11–14}

YEATS domains are newly identified epigenetic “readers” that recognize histone lysine acetylation (Kac) and crotonylation (Kcr) via conserved aromatic “sandwich” cages.^{15–19} The human genome encodes four YEATS domain-containing proteins, AF9, ENL, GAS41, and YEATS2, which exist in multiple chromatin-remodeling and histone-modifying complexes.²⁰ Given the critical roles played by these complexes in gene regulation and chromatin biology, aberrant YEATS-dependent readouts of histone modifications have been associated with the pathogenesis and progression of human diseases, such as cancer.^{21–24} These discoveries suggest that YEATS domains are promising drug targets.

We recently developed the first class of peptide-based YEATS domain inhibitors with submicromolar activity by targeting a unique π – π – π stacking that underlies the YEATS–Kcr recognition (Figure S1).²⁵ The high affinity between the YEATS domains and our inhibitors was achieved by replacing the original crotonyl group with expanded π systems to enhance the π – π – π stacking interactions (e.g., furan in XL-07i and oxazole in XL-13a, Figure 1A). Research by others has also led to the identification of a set of small molecule YEATS inhibitors.^{26–29}

The reported inhibitors showed a general preference toward the YEATS domains of AF9 and its paralog ENL, which are known to participate in the regulation of gene transcription by serving as a member of transcriptional complexes, for example, the super elongation complex (SEC).³⁰ While it is clear that the presence of these two paralogs in one complex is mutually exclusive,³¹ the different roles played by either AF9- or ENL-containing complexes in specific gene regulation events have been poorly understood. The development of selective

Received: October 5, 2020



ACS Publications

© XXXX American Chemical Society

A

<https://dx.doi.org/10.1021/jacs.0c10324>
J. Am. Chem. Soc. XXXX, XXX, XXX–XXX

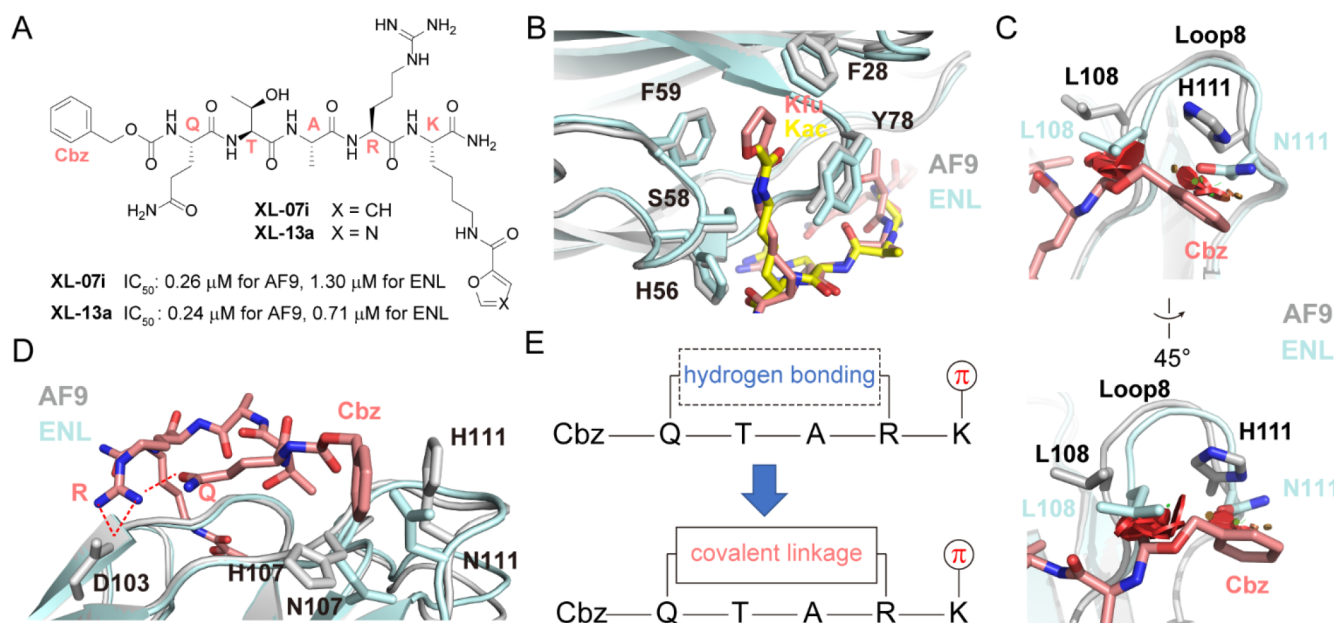


Figure 1. Development of cyclopeptide inhibitors selective for AF9 YEATS domain. (A) Structures and inhibitory activities of previously reported YEATS inhibitors XL-07i and XL-13a. (B) Superimposition of structures of AF9 YEATS–XL-07i (PDB: 5YYF) and ENL YEATS–H3K27ac (PDB: 5J9S) complexes in their acyllysine-binding pockets. (C) Steric clash between the Cbz group of XL-07i and the Loop 8 surface of ENL YEATS. Small to large and green to red disks indicate slight to significant steric interactions. (D) XL-07i forms different contacts with AF9 YEATS. Cbz is involved in different π stackings with H107 and H111 of AF9 but not with N107 and N111 of ENL. Red dash lines indicate hydrogen bonding. (E) Design strategy of the cyclopeptide inhibitors.

inhibitors should provide useful tools to functionally distinguish isoforms of transcriptional complexes containing either AF9 or ENL. However, it is extremely challenging to pursue the selectivity between AF9 and ENL YEATS, as the residues that shape the acyllysine-binding pockets in these two domains are identical (Figure 1B).

We reasoned that targeting an additional site outside the acyllysine-binding pocket would be a solution to increase the inhibitor selectivity. Here, we describe the identification of a site proximal to the acyllysine-binding pocket that distinguishes AF9 YEATS from ENL YEATS. By developing cyclopeptide inhibitors with preorganized conformation that target both the acyllysine pocket and the proximal site, we achieved selective inhibition of the AF9 YEATS domain. The most selective inhibitor, JYX-3, showed a 38-fold higher binding affinity toward AF9 YEATS over ENL YEATS.

RESULTS AND DISCUSSION

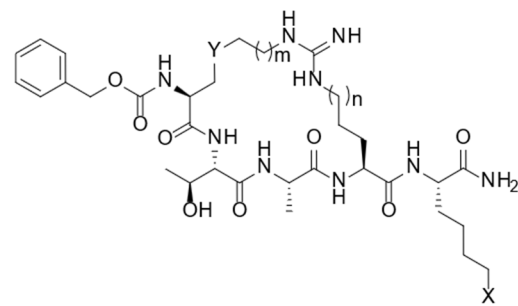
Development of AF9 YEATS-Selective Cyclopeptide Inhibitors. In our previous study, we developed two potent pentapeptide inhibitors, XL-07i and XL-13a, which showed slightly higher selectivity for AF9 YEATS over ENL YEATS (3–5 folds, Figure 1A).²⁵ To uncover the different binding behaviors between AF9 and ENL YEATS on interacting with XL-07i and XL-13a, we superposed the crystal structure of ENL YEATS bound to a histone H3K27ac peptide over the structure of the AF9 YEATS–XL-07i complex. Although the acyllysine-binding pockets of these two proteins are well-aligned (Figure 1B), the surface at the Loop 8 region of ENL YEATS, mainly the L108 and N111 side-chains, clashed with the XL-07i N-terminal carboxybenzyl (Cbz) group (Figure 1C). Similar incompatibles were also observed when the *apo* ENL YEATS or ENL YEATS in complex with an acetylated lysine were superposed with AF9 YEATS–XL-07i (Figure S2). On the contrary, the Cbz group of XL-07i was favored by AF9

YEATS as it formed different π stackings with the imidazole rings of AF9 H107 and H111 residues (Figure 1D).²⁵ Notably, these two positions in ENL are Asn instead of His, indicating the absence of the π stackings in this region of ENL. Taken together, inhibitors with proper functional groups approaching the Loop 8 region in YEATS domains should show selectivity between AF9 and ENL.

We noticed that, to place its Cbz group in the Loop 8 region of AF9 YEATS, XL-07i peptide adopted a constrained conformation by forming an intramolecular hydrogen bond between the amide carbonyl group on the side-chain of Gln and the guanidine proton of Arg (Figure 1D). We reasoned that cyclization of the original linear peptides by replacing the hydrogen bond with covalent linkages could rigidify the inhibitors into the AF9 YEATS-favored conformation (Figure 1E). On the basis of the structures of XL-07i and XL-13a, we first developed four cyclopeptide inhibitors (JYX-1–JYX-4, Table 1) carrying either a furan or an oxazole ring at the lysine side chain. The original amide of Gln was removed, and the alkyl chain was covalently linked to the guanido group. The guanidine was retained as it contributed to the YEATS–inhibitor interaction by forming a charge stabilized hydrogen bond with AF9 D103 (Figure 1D). An inhibitor lacking the conjugated π system (JYX-0) at the lysine side-chain was also prepared as an inactive control.

We adopted a fluorescence-based competitive photo-cross-linking assay^{25,32,33} to estimate the inhibitory activity of these four cyclopeptides on AF9 YEATS (Figure S3A). As shown in Figure 2A, all of the four inhibitors could efficiently block the interaction between AF9 YEATS and a crotonylated peptide probe 1 (Figure S3B). Specifically, JYX-3 (IC₅₀ = 0.41 μM) and JYX-4 (IC₅₀ = 0.56 μM) exhibited higher potencies than JYX-1 (IC₅₀ = 1.78 μM) and JYX-2 (IC₅₀ = 2.23 μM), which was consistent with our previous result that the oxazole ring was preferred by AF9 YEATS compared with the furan ring.²⁵

Table 1. Structures of JYX-0 to JYX-8 and Their Inhibitory Activity toward AF9 and ENL YEATS Domains



Compound No.	X	Y	m	n	AF9 IC ₅₀ (μM)	ENL IC ₅₀ (μM)	AF9/ENL selectivity (folds)
JYX-0	H	H ₂ C	1	1	Inactive	Inactive	/
JYX-1		H ₂ C	1	1	1.78	43.64	24.5
JYX-2		H ₂ C	1	2	2.23	14.53	6.5
JYX-3		H ₂ C	1	1	0.41	12.80	31.2
JYX-4		H ₂ C	1	2	0.56	10.84	19.4
JYX-5		S	1	1	0.83	14.30	17.2
JYX-6			1	1	2.19	15.50	7.1
JYX-7			1	1	8.33	7.11	0.9
JYX-8			0	1	5.05	9.02	1.8

More importantly, **JYX-3** and **JYX-4** showed 31-fold and 19-fold decreased inhibitory activity on ENL YEATS (**JYX-3**, IC₅₀ = 12.80 μM; **JYX-4**, IC₅₀ = 10.84 μM) than that on AF9 YEATS, respectively (Figure 2B), indicating a substantially increased selectivity toward AF9 over ENL compared with the linear precursor **XL-13a** (only 3 folds). As expected, the negative control inhibitor **JYX-0** showed no affinity to either AF9 or ENL YEATS as it failed to compete the probe-1-induced labeling toward these two domains (Figure S4).

We next examined the selectivity of **JYX-3** against a panel of epigenetic regulators (Figures S5–S8), including another two human YEATS domains (GAS41 and YEATS2),²⁵ canonical Kac “readers” (bromodomains of BRD2(2), BRD3(2), BRD4(1), BRD4(2), BRD9, TAF1(2), and CECR2),³⁴ lysine acylation “erasers” (Sirt2, Sirt3, Sirt5, and Sirt6),^{35,36} and histone methylation “readers” (ING2 and SPIN1).³⁵ **JYX-3** showed little inhibitory effects toward all the tested proteins. Further trials to diversify the covalent linkages (**JYX-5**–**JYX-8**) that cyclized the inhibitors revealed that a simple 4-carbon chain (as in **JYX-3**) was the best linker among all the tested

ones (Table 1 and Figure S9). The introduction of any moiety into the carbon chain would diminish the inhibitor selectivity for AF9 YEATS.

Structural Features in the Loop 8 Region of AF9 YEATS Underlie the Inhibitor Selectivity. To study the molecular basis of how the cyclopeptide engages with AF9 YEATS, we determined the crystal structure of AF9 YEATS in complex with **JYX-3** at 3.05 Å resolution (Figure 3A and Table S1). In the complex, **JYX-3** exhibits an almost identical binding pose to that of its linear counterpart **XL-07i**. Similar to **XL-07i/13a**, **JYX-3** also keeps all the key features critical for AF9 YEATS binding, including Koxa-accommodating hydrogen bonding and hydrophobic interactions, guanido group-D103 hydrogen bonding, and π stacking interactions between Cbz and H107 and H111 side-chains (Figure 3A,B). Compared with **XL-07i**, there is a highly coordinated hydrogen bonding network involving AF9 D103, the Gln side-chain amide of **XL-07i**, and a structural water molecule not seen for **JYX-3** (Figure S10), which might account for the slightly reduced inhibitory

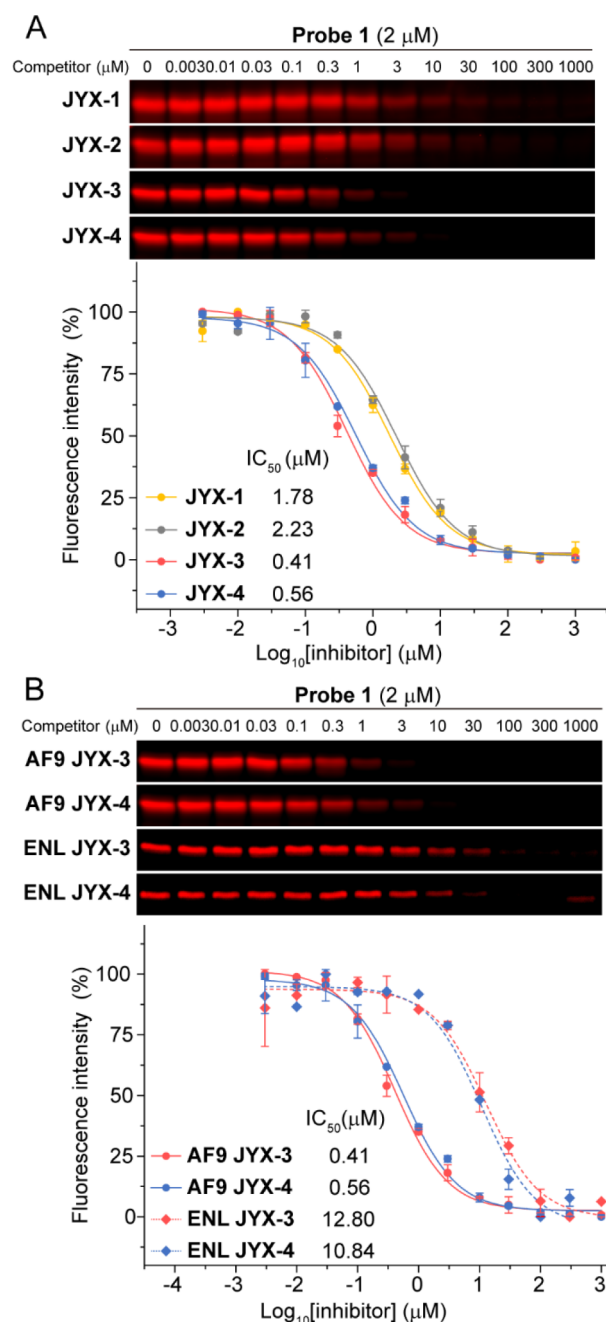


Figure 2. Determination of inhibitory activity of cyclopeptide inhibitors toward AF9 and ENL YEATS domains. (A and B) Competitive photo-cross-linking assay to determine the inhibitory activities of the cyclopeptides JYX-1 to JYX-4 toward AF9 YEATS (A) and JYX-3 and JYX-4 toward AF9 and ENL YEATS, respectively (B). Protein concentration was 5 $\mu\text{g}/\text{mL}$. After photo-cross-linking, the probe-1-labeled proteins were conjugated to rhodamine- N_3 and visualized by in-gel fluorescence scanning. All curves were normalized between 100% and 0% at the highest and lowest fluorescence intensities, respectively. Data are reported as mean \pm s.d., $n = 2$.

activity of JYX-3 ($\text{IC}_{50} = 0.41 \mu\text{M}$) than XL-13a ($\text{IC}_{50} = 0.24 \mu\text{M}$) toward AF9 YEATS.

To gain more insight into how interactions between the Cbz group and the Loop 8 of AF9 YEATS contributed to the selectivity of the cyclopeptide inhibitors, we further synthesized a collection of JYX-3 analogues (JYX-9–JYX-33) with the Cbz substituted by different functional groups. The

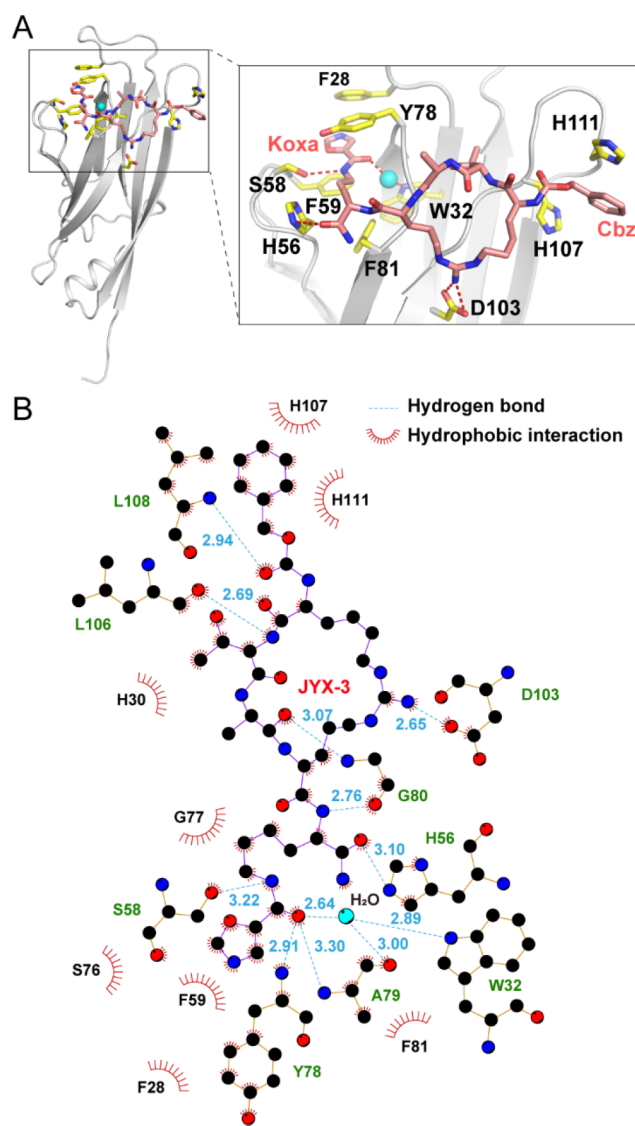
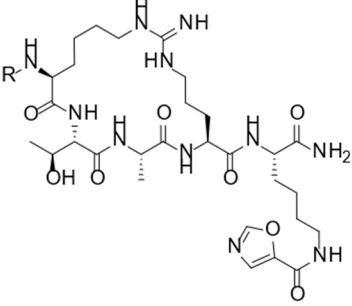


Figure 3. Crystal structure of AF9 YEATS domain in complex with JYX-3. (A) Overall structure of AF9 YEATS (gray) bound to JYX-3 (salmon). Key AF9 residues (yellow) accommodating the inhibitor are highlighted. (B) Two-dimensional interaction diagram of JYX-3 with AF9 YEATS. Numbers show the distances of the indicated hydrogen bonds in Å.

assessment of the inhibitory activities of these cyclopeptides (Table 2 and Figure S11) revealed that the inhibitors' selectivity was indeed sensitive to structural changes of the moieties in contact with the Loop 8. Specifically, AF9 YEATS tolerated a broad spectrum of changes at this site, while ENL YEATS disfavored almost any substitutions larger than acetyl in size. By casting a careful glance at the Loop 8 of ENL YEATS, the overall structure is firmly stabilized by multiple intramolecular hydrogen bonds (Figure 4A), which make the loop too rigid to host any foreign ligands requiring conformational changes. In contrast, the Loop 8 of AF9 YEATS is likely to be more flexible to accommodate guests as it only involves one hydrogen bond. When the linear peptide inhibitor, XL-13a, approaches ENL YEATS, it is easy for the peptide to adopt conformational changes to avoid direct clashes between the Cbz group and the Loop 8 of the protein. After cyclization, the conformation of the inhibitor has been fixed, the rigidity of both the cyclopeptide and the Loop 8 of ENL YEATS

Table 2. Structures of JYX-9 to JYX-33 and Their Inhibitory Activity toward AF9 and ENL YEATS Domains



Compound No.	R	AF9 IC ₅₀ (μM)	ENL IC ₅₀ (μM)	AF9/ENL selectivity (folds)	Compound No.	R	AF9 IC ₅₀ (μM)	ENL IC ₅₀ (μM)	AF9/ENL selectivity (folds)
JYX-3		0.41	12.80	31.2	JYX-21		1.53	13.33	8.7
JYX-9	H	32.61	37.62	1.2	JYX-22		0.62	14.83	23.8
JYX-10		4.02	9.02	2.2	JYX-23		1.57	12.41	7.9
JYX-11		1.49	12.00	8.1	JYX-24		1.65	12.96	7.9
JYX-12		0.98	12.55	12.8	JYX-25		1.96	21.11	10.8
JYX-13		0.73	13.36	18.4	JYX-26		1.37	9.47	6.9
JYX-14		7.76	116.40	15.0	JYX-27		4.55	17.64	3.9
JYX-15		1.57	20.85	13.2	JYX-28		2.42	11.33	4.7
JYX-16		1.29	18.93	14.7	JYX-29		1.59	12.58	7.9
JYX-17		2.00	11.09	5.5	JYX-30		1.11	8.62	7.8
JYX-18		4.72	14.44	3.1	JYX-31		2.23	10.93	4.7
JYX-19		2.27	22.23	9.8	JYX-32		1.89	27.59	14.6
JYX-20		1.19	13.49	11.3	JYX-33		1.12	16.93	15.1

eventually lead to a substantial decrease in their binding affinity, and therefore, increase the selectivity of the cyclopeptide toward AF9 YEATS.

On the contrary, the Cbz group in JYX-3 seemed not to be simply accommodated by the Loop 8 of AF9 YEATS but provided key interactions with the protein by it forming additional π stackings with H107 and H111, respectively

(Figure 3A,B). Indeed, the two corresponding residues in ENL YEATS turned out to be asparagine (N107 and N111), which also are the only two residues that differ AF9 YEATS from ENL YEATS in their Loop 8 regions (Figure 4A). To further investigate the contribution of the Cbz-mediated π interactions to the selectivity, we generated AF9 and ENL YEATS mutants with their 107 and 111 residues swapped, i.e., the H107N and

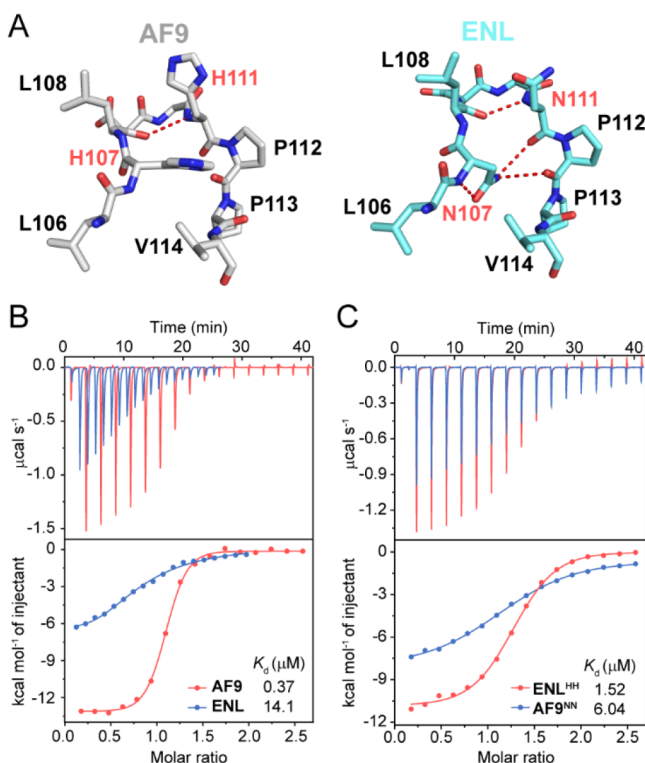


Figure 4. Structure features of AF9 YEATS Loop 8 underlie the inhibitor selectivity. (A) Loop 8 region of ENL YEATS is more rigidified than that of AF9. (B and C) ITC measurements for the binding affinities of JYX-3 with AF9 and ENL YEATS (B) and AF9^{NN} and ENL^{HH} mutants (C).

H111N dual mutations in AF9 (AF9^{NN}) and N107H and N111H dual mutations in ENL (ENL^{HH}). Isothermal titration calorimetry (ITC) measurements showed that JYX-3 had a 38-fold binding preference for AF9 YEATS ($K_d = 0.37 \mu\text{M}$) over ENL YEATS ($K_d = 14.1 \mu\text{M}$), while the K_d values of the same inhibitor toward AF9^{NN} and ENL^{HH} were 6.04 and 1.52 μM , respectively (Figure 4B,C and Table S2). Compared with their wild-type counterparts, the 16-fold affinity drop of AF9^{NN} and 9-fold binding enhancement of ENL^{HH} to JYX-3 completely reversed their preference toward the cyclopeptide inhibitor. Taken together, investigations by changing the structure features of either the cyclopeptides or the YEATS domains strongly suggested that the Cbz-His-His unit in the Loop 8 region should be a main contributor to the selectivity of JYX-3 toward AF9 YEATS.

JYX-3 Is Cell Permeable and Selectively Engages with Endogenous AF9. We next monitored the engagement of JYX-3 with endogenous AF9. To this end, HeLa S3 nuclear extracts were photo-cross-linked with the **probe 1** in the presence of JYX-3. The **probe-1**-labeled and thus enriched proteins were subjected to immunoblotting analysis against anti-AF9 and anti-ENL antibodies. In the presence of 2 μM JYX-3, 60% enrichment of endogenous AF9 was blocked while the enrichment of ENL left unaffected (Figure 5A,B). At 20 μM , JYX-3 inhibited more than 90% AF9 enrichment, while the enrichment of ENL was still as much as 60%. This result revealed that, at the endogenous protein level, JYX-3 also showed satisfactory AF9 selectivity.

Encouraged by the *in vitro* results, we proceeded to examine the performance of JYX-3 in living cells. Using the immobilized artificial membrane (IAM) chromatography³⁷ and the parallel

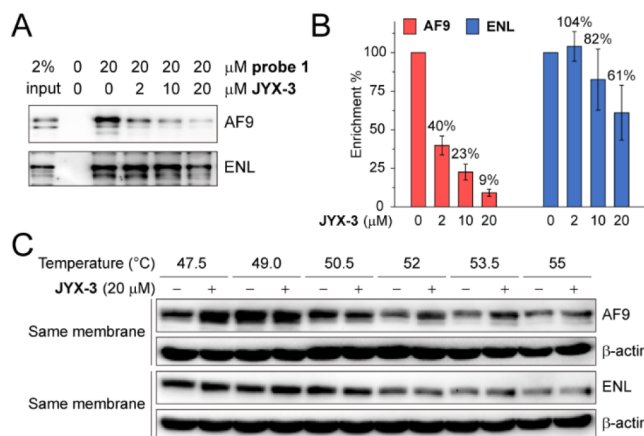


Figure 5. JYX-3 is selective for endogenous AF9. (A) Photo-cross-linking pull-down in nuclear extracts (1 mg/mL) with **probe 1** in the presence or absence of JYX-3. After photo-cross-linking, the **probe-1**-labeled proteins were conjugated to biotin-N₃ and enriched by streptavidin. The eluted protein mixtures were analyzed by immunoblotting. (B) Quantification of the inhibitory effects of JYX-3 on the enrichment of AF9 and ENL in (A). Data are reported as mean \pm s.d. ($n = 3$). (C) CETSA to show the engagement of JYX-3 with endogenous AF9, but not ENL, in living cells. HeLa cells treated with or without JYX-3 were heated at indicated temperatures. The soluble proteins were analyzed by immunoblotting. β -Actin was used as a loading control. Each blotting in (A) and (C) is representative of three independent experiments.

artificial membrane permeability assay (PAMPA),³⁸ we first demonstrated that the cyclization indeed increased the lipophilicity and passive transport rate of the inhibitor (Figures S12 and S13). Although there would still be a large space to improve, JYX-3 behaved comparably to theophylline, a model drug known to have relatively low cell membrane permeability.³⁹ In addition, JYX-3 exhibited a higher stability than its linear precursor XL-13a (Figure S14). We next applied the cellular thermal shift assay (CETSA)^{40,41} to determine whether JYX-3 could target AF9 in living cells. HeLa cells treated with or without 20 μM JYX-3 were heated at different temperatures. Soluble proteins were then extracted and analyzed by immunoblotting. As expected, JYX-3 helped AF9 resist the high-temperature-induced denaturation, while the thermal stability of ENL remained unchanged upon the inhibitor treatment (Figure 5C). The CETSA results indicated that JYX-3 could traverse the cell membrane and selectively engage with the endogenous AF9, but not ENL, under the tested conditions.

JYX-3 Disrupts the Chromatin Association of AF9 and Downregulates the Expression of AF9 Target Genes. To assess the ability of JYX-3 to inhibit the chromatin association of AF9, we performed a fluorescence recovery after photo-bleaching (FRAP) assay⁴² using U2OS cells transfected with a full-length AF9 fused with GFP. A significant increase in the fluorescence recovery rate was observed when the cells were treated with JYX-3, which phenocopied the loss-of-Kac-binding AF9 mutant (F59A) (Figure 6A–C). The increased mobility of AF9–GFP was, therefore, likely to arise from the displacement of AF9 YEATS from the acetylated chromatin by JYX-3. FRAP using ENL–GFP, however, showed no differences in the recovery rates acquired from samples in the presence and absence of JYX-3 (Figure 6D–F), further supporting the AF9 selectivity of the inhibitor in cellular environment.

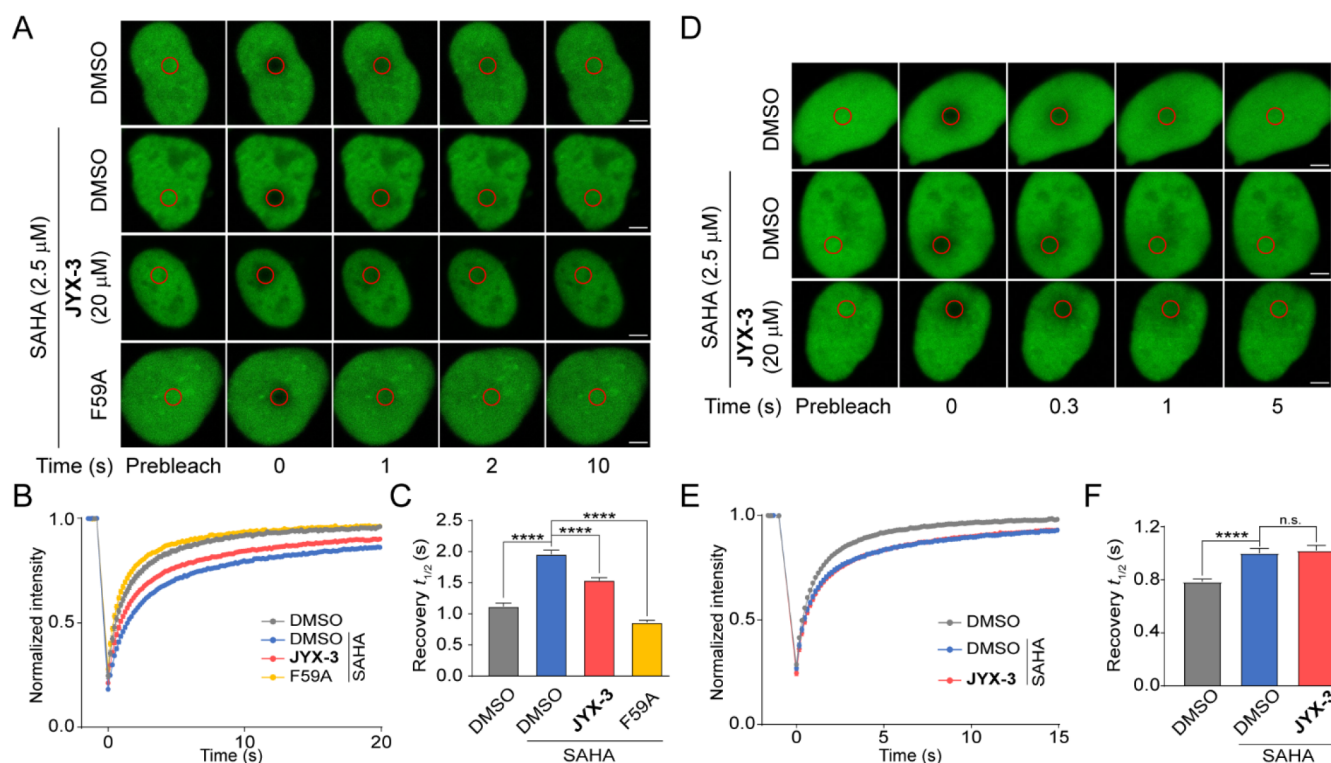


Figure 6. JYX-3 disrupts the YEATS-dependent chromatin association of AF9. (A) FRAP assay using AF9–GFP. (B and C) FRAP curves (B) and recovery $t_{1/2}$ (C) of each group in (A). (D) FRAP assay using ENL–GFP. (E and F) FRAP curves (E) and recovery $t_{1/2}$ (F) of each group in (D). In (A) and (D), shown are the representative nuclei of transfected U2OS cells pre- or postbleaching at indicated time points. Red circles indicate the bleached regions. The pan-HDAC inhibitor SAHA was used to increase the global Kac level.⁴² Scale bar = 4 μ m. Data are reported as mean \pm s.e.m., $n \geq 20$. P values are based on the two-tailed Student's t -test. **** $P < 0.0001$, n.s.: not significant.

We next sought out to explore the effects of JYX-3 on the AF9 YEATS-dependent regulation of gene expression. The YEATS domain is known to be essential for the enrichment of AF9 at its target genes, for example, *MYC* and *PABPC1*.⁴³ AF9 may further recruit histone H3K79 methyltransferase DOT1L, leading to elevated H3K79 dimethylation (Kme2) or trimethylation (Kme3) levels and transcription activation of the target genes. By performing chromatin immunoprecipitation and quantitative PCR (ChIP-qPCR) in HeLa cells, we detected reduced abundances of AF9 and H3K79me3, but not ENL, on *MYC* and *PABPC1* upon JYX-3 treatment (Figure 7A), suggesting that the cyclopeptide could disrupt the YEATS-dependent enrichment of AF9 on its target genes and could further prevent the recruitment of DOT1L. In addition, the exposure of HeLa cells to JYX-3 induced significant losses in the transcription levels of *MYC* and *PABPC1* (Figure 7B), which was in good accordance with the unloading of AF9 from these two genes. Our observations agree with the previous discoveries that AF9 downregulation or Kac-binding-impaired mutations in AF9 YEATS led to transcription defects of its target genes.⁴³

CONCLUSION

In summary, we developed the first AF9 YEATS domain-specific inhibitor with 38-fold or higher selectivity over ENL and other human YEATS domains. The selectivity of the inhibitor is achieved by preorganizing the conformation of a previously reported peptide-based inhibitor *via* structure-guided cyclization, which places a Cbz group to the Loop 8 region of YEATS domains. Such conformation is only favored by the Loop 8 of AF9 YEATS, in which the H107 and H111

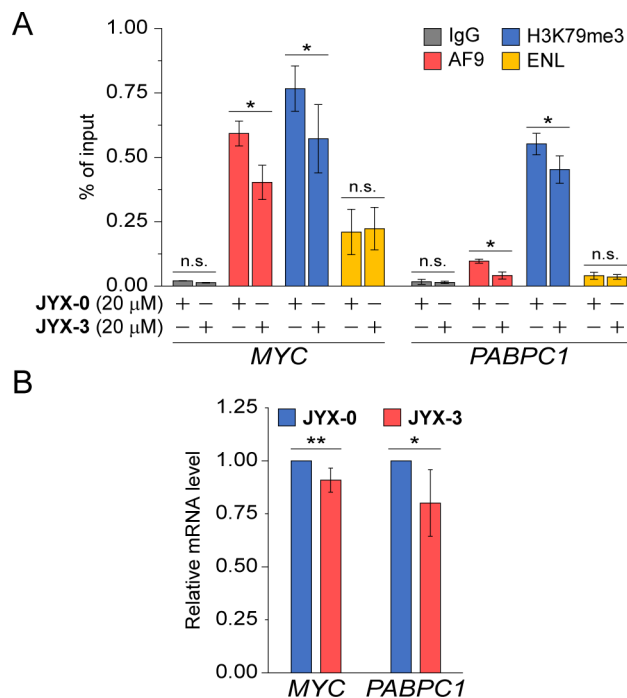


Figure 7. JYX-3 perturbs the YEATS-dependent gene regulation activity of AF9. (A) ChIP-qPCR analysis of AF9 target genes in HeLa cells treated with inhibitors. (B) RT-qPCR analysis shows mRNA levels of AF9 target genes in HeLa cells treated with inhibitors (20 μ M). Data are presented as mean \pm s.e.m., $n \geq 3$. P values are based on the two-tailed Student's t -test. * $P < 0.05$, ** $P < 0.01$, n.s.: not significant.

residues form extensive π stacking interactions with the Cbz. These interactions are absent in other YEATS domains as their corresponding histidine positions are substituted with non-aromatic amino acids. The development of selective YEATS domain inhibitors has been challenging as the acyllysine-binding pockets of all YEATS domain are highly conserved. Our study provides a novel strategy to realize the selectivity by targeting an additional site outside the acyllysine-binding pocket that distinguishes one YEATS from another. We envision that similar methods can also be used to develop inhibitors selective for YEATS domains of ENL, YEATS2, and GAS41, as well as other structurally conserved epigenetic “readers”, such as bromodomain and chromodomain.^{44,45}

■ ASSOCIATED CONTENT

SI Supporting Information

The Supporting Information is available free of charge at <https://pubs.acs.org/doi/10.1021/jacs.0c10324>.

Figures of complex structures, superimposition of structures, schematic diagram illustrating the competitive photo-cross-linking assay, in-gel fluorescence scanning, in-gel fluorescence and competition curves, IAM chromatography analysis, PAMPA analysis of the inhibitors, and stability analysis of the inhibitors, tables of data collection and refinement statistics and ITC thermodynamic parameters of different YEATS domains, discussions of reagents, antibodies, and instrumentation used, molecular cloning, protein expression, and purification, cell culture, preparation of nuclear extracts, photo-cross-linking, Cu(I)-catalyzed azide-alkyne cycloaddition/click chemistry, in-gel fluorescence scanning, isothermal titration calorimetry measurements, immunoblotting, chromatin immunoprecipitation and quantitative PCR, quantitative PCR analysis, cellular thermal shift assay, fluorescence recovery after photobleaching, immobilized artificial membrane chromatography, parallel artificial membrane permeability assay, stability test of inhibitors, crystallization, design, synthesis, and characterization of photoaffinity probes, synthesis methods used, and data strings, schemes of synthetic pathways and LC–MS spectra (PDF)

■ AUTHOR INFORMATION

Corresponding Authors

Yuanyuan Li – MOE Key Laboratory of Protein Sciences, Beijing Advanced Innovation Center for Structural Biology, Beijing Frontier Research Center for Biological Structure, Department of Basic Medical Sciences, School of Medicine and Tsinghua-Peking Center for Life Sciences, Tsinghua University, Beijing 100084, China; Email: liyuan@tsinghua.edu.cn

Xin Li – Departments of Chemistry, The University of Hong Kong, Hong Kong, China; orcid.org/0000-0001-9698-1883; Email: lx418@hku.hk

Haitao Li – MOE Key Laboratory of Protein Sciences, Beijing Advanced Innovation Center for Structural Biology, Beijing Frontier Research Center for Biological Structure, Department of Basic Medical Sciences, School of Medicine and Tsinghua-Peking Center for Life Sciences, Tsinghua University, Beijing 100084, China; Email: lht@tsinghua.edu.cn

Xiang David Li – Departments of Chemistry, The University of Hong Kong, Hong Kong, China; orcid.org/0000-0002-2797-4134; Email: xiangli@hku.hk

Authors

Yixiang Jiang – Departments of Chemistry, The University of Hong Kong, Hong Kong, China

Guochao Chen – MOE Key Laboratory of Protein Sciences, Beijing Advanced Innovation Center for Structural Biology, Beijing Frontier Research Center for Biological Structure, Department of Basic Medical Sciences, School of Medicine and Tsinghua-Peking Center for Life Sciences, Tsinghua University, Beijing 100084, China

Xiao-Meng Li – Departments of Chemistry, The University of Hong Kong, Hong Kong, China

Sha Liu – Departments of Chemistry, The University of Hong Kong, Hong Kong, China

Gaofer Tian – Departments of Chemistry, The University of Hong Kong, Hong Kong, China

Complete contact information is available at: <https://pubs.acs.org/doi/10.1021/jacs.0c10324>

Author Contributions

[†]Y.J., G.C., and X.-M.L. contributed equally to this work.

Notes

The authors declare the following competing financial interest(s): X.L. and X.D.L. are co-inventors on a patent (Publication No. WO 2019/101195) related to the cyclopeptide inhibitors reported in this manuscript.

■ ACKNOWLEDGMENTS

The authors would like to acknowledge the support from National Natural Science Foundation of China (91753203 to X.D.L. and H.L., 91753130 to X.D.L., 31725014 to H.L., and 31871283 and 31922016 to Y.L.), Excellent Young Scientists Fund of China (Hong Kong and Macau) (21922708 to X.D.L.), National Key R&D Program of China (2020YFA0803300 to H.L.), Beijing Natural Science Foundation (5182014 to Y.L.), Beijing Metropolis for the Beijing Nova Program (Z181100006218068 to Y.L.), and China Association for Science and Technology for the Young Elite Scientists Sponsorship Program (YESS20170075 to Y.L.). The authors would like to acknowledge the support from the Hong Kong Research Grants Council (RGC) Collaborative Research Fund (CRF C7029-15G and C7017-18G to X.D.L.), the Areas of Excellence Scheme (AoE/P-705/16 to X.D.L.), the General Research Fund (GRF 17121120, 17126618, and 17125917 to X.D.L.), and the RGC Postdoctoral Fellowship (Scheme 2020/21 to X.L.). Y.L. is a Tsinghua Advanced Innovation Young Scientist. The authors would like to thank the staff members at beamline BL17U1 of Shanghai Synchrotron Radiation Facility and Dr. S.F. at Tsinghua Center for Structural Biology for their assistance in data collection and the China National Center for Protein Sciences Beijing for providing facility support.

■ REFERENCES

- (1) Manning, G.; Whyte, D. B.; Martinez, R.; Hunter, T.; Sudarsanam, S. The protein kinase complement of the human genome. *Science* **2002**, 298 (5600), 1912–1934.
- (2) Levitzki, A. Protein kinase inhibitors as a therapeutic modality. *Acc. Chem. Res.* **2003**, 36 (6), 462–469.

- (3) Fabian, M. A.; Biggs, W. H., 3rd; Treiber, D. K.; Atteridge, C. E.; Azimioara, M. D.; Benedetti, M. G.; Carter, T. A.; Ciceri, P.; Edeen, P. T.; Floyd, M.; Ford, J. M.; Galvin, M.; Gerlach, J. L.; Grotzfeld, R. M.; Herrgard, S.; Insko, D. E.; Insko, M. A.; Lai, A. G.; Lelias, J. M.; Mehta, S. A.; Milanov, Z. V.; Velasco, A. M.; Wodicka, L. M.; Patel, H. K.; Zarrinkar, P. P.; Lockhart, D. J. A small molecule-kinase interaction map for clinical kinase inhibitors. *Nat. Biotechnol.* **2005**, *23* (3), 329–336.
- (4) Davis, M. I.; Hunt, J. P.; Herrgard, S.; Ciceri, P.; Wodicka, L. M.; Pallares, G.; Hocker, M.; Treiber, D. K.; Zarrinkar, P. P. Comprehensive analysis of kinase inhibitor selectivity. *Nat. Biotechnol.* **2011**, *29* (11), 1046–1051.
- (5) Anastassiadis, T.; Deacon, S. W.; Devarajan, K.; Ma, H.; Peterson, J. R. Comprehensive assay of kinase catalytic activity reveals features of kinase inhibitor selectivity. *Nat. Biotechnol.* **2011**, *29* (11), 1039–1045.
- (6) Bantscheff, M.; Eberhard, D.; Abraham, Y.; Bastuck, S.; Boesche, M.; Hobson, S.; Mathieson, T.; Perrin, J.; Raida, M.; Rau, C.; Reader, V.; Sweetman, G.; Bauer, A.; Bouwmeester, T.; Hopf, C.; Kruse, U.; Neubauer, G.; Ramsden, N.; Rick, J.; Kuster, B.; Drewes, G. Quantitative chemical proteomics reveals mechanisms of action of clinical ABL kinase inhibitors. *Nat. Biotechnol.* **2007**, *25* (9), 1035–1044.
- (7) Karaman, M. W.; Herrgard, S.; Treiber, D. K.; Gallant, P.; Atteridge, C. E.; Campbell, B. T.; Chan, K. W.; Ciceri, P.; Davis, M. I.; Edeen, P. T.; Faraoni, R.; Floyd, M.; Hunt, J. P.; Lockhart, D. J.; Milanov, Z. V.; Morrison, M. J.; Pallares, G.; Patel, H. K.; Pritchard, S.; Wodicka, L. M.; Zarrinkar, P. P. A quantitative analysis of kinase inhibitor selectivity. *Nat. Biotechnol.* **2008**, *26* (1), 127–132.
- (8) Shi, H.; Zhang, C. J.; Chen, G. Y.; Yao, S. Q. Cell-based proteome profiling of potential dasatinib targets by use of affinity-based probes. *J. Am. Chem. Soc.* **2012**, *134* (6), 3001–3014.
- (9) Zhao, Q.; Ouyang, X.; Wan, X.; Gajiwala, K. S.; Kath, J. C.; Jones, L. H.; Burlingame, A. L.; Taunton, J. Broad-Spectrum Kinase Profiling in Live Cells with Lysine-Targeted Sulfonyl Fluoride Probes. *J. Am. Chem. Soc.* **2017**, *139* (2), 680–685.
- (10) Knight, Z. A.; Lin, H.; Shokat, K. M. Targeting the cancer kinome through polypharmacology. *Nat. Rev. Cancer* **2010**, *10* (2), 130–137.
- (11) Lamba, V.; Ghosh, I. New Directions in Targeting Protein Kinases: Focusing Upon True Allosteric and Bivalent Inhibitors. *Curr. Pharm. Des.* **2012**, *18* (20), 2936–2945.
- (12) Zhan, P.; Itoh, Y.; Suzuki, T.; Liu, X. Y. Strategies for the Discovery of Target-Specific or Isoform-Selective Modulators. *J. Med. Chem.* **2015**, *58* (19), 7611–7633.
- (13) van Wandelen, L. T. M.; van Ameijde, J.; Ismail-Ali, A. F.; van Ufford, H. C. Q.; Vijftingschild, L. A. W.; Beekman, J. M.; Martin, N. I.; Ruijtenbeek, R.; Liskamp, R. M. J. Cell-Penetrating Bisubstrate-Based Protein Kinase C Inhibitors. *ACS Chem. Biol.* **2013**, *8* (7), 1479–1487.
- (14) van Wandelen, L. T.; van Ameijde, J.; Mady, A. S.; Wammes, A. E.; Bode, A.; Poot, A. J.; Ruijtenbeek, R.; Liskamp, R. M. Directed modulation of protein kinase C isozyme selectivity with bisubstrate-based inhibitors. *ChemMedChem* **2012**, *7* (12), 2113–2121.
- (15) Li, Y.; Wen, H.; Xi, Y.; Tanaka, K.; Wang, H.; Peng, D.; Ren, Y.; Jin, Q.; Dent, S. Y.; Li, W.; Li, H.; Shi, X. AF9 YEATS domain links histone acetylation to DOT1L-mediated H3K79 methylation. *Cell* **2014**, *159* (3), 558–571.
- (16) Li, Y.; Sabari, B. R.; Panchenko, T.; Wen, H.; Zhao, D.; Guan, H.; Wan, L.; Huang, H.; Tang, Z.; Zhao, Y.; Roeder, R. G.; Shi, X.; Allis, C. D.; Li, H. Molecular Coupling of Histone Crotonylation and Active Transcription by AF9 YEATS Domain. *Mol. Cell* **2016**, *62* (2), 181–193.
- (17) Andrews, F. H.; Shinsky, S. A.; Shanley, E. K.; Bridgers, J. B.; Gest, A.; Tsun, I. K.; Krajewski, K.; Shi, X. B.; Strahl, B. D.; Kutateladze, T. G. The Taf14 YEATS domain is a reader of histone crotonylation. *Nat. Chem. Biol.* **2016**, *12* (6), 396–398.
- (18) Zhao, D.; Guan, H. P.; Zhao, S.; Mi, W. Y.; Wen, H.; Li, Y. Y.; Zhao, Y. M.; Allis, C. D.; Shi, X. B.; Li, H. T. YEATS2 is a selective histone crotonylation reader. *Cell Res.* **2016**, *26* (5), 629–632.
- (19) Zhang, Q.; Zeng, L.; Zhao, C. C.; Ju, Y.; Konuma, T.; Zhou, M. M. Structural Insights into Histone Crotonyl-Lysine Recognition by the AF9 YEATS Domain. *Structure* **2016**, *24* (9), 1606–1612.
- (20) Schulze, J. M.; Wang, A. Y.; Kobor, M. S. YEATS domain proteins: a diverse family with many links to chromatin modification and transcription. *Biochem. Cell Biol.* **2009**, *87* (1), 65–75.
- (21) Wan, L. L.; Wen, H.; Li, Y. Y.; Lyu, J.; Xi, Y. X.; Hoshii, T.; Joseph, J. K.; Wang, X. L.; Loh, Y. H. E.; Erb, M. A.; Souza, A. L.; Bradner, J. E.; Shen, L.; Li, W.; Li, H. T.; Allis, C. D.; Armstrong, S. A.; Shi, X. B. ENL links histone acetylation to oncogenic gene expression in acute myeloid leukaemia. *Nature* **2017**, *543* (7644), 265–269.
- (22) Erb, M. A.; Scott, T. G.; Li, B. E.; Xie, H. F.; Paulk, J.; Seo, H. S.; Souza, A.; Roberts, J. M.; Dastjerdi, S.; Buckley, D. L.; Sanjana, N. E.; Shalem, O.; Nabet, B.; Zeid, R.; Offei-Addo, N. K.; Dhe-Paganon, S.; Zhang, F.; Orkin, S. H.; Winter, G. E.; Bradner, J. E. Transcription control by the ENL YEATS domain in acute leukaemia. *Nature* **2017**, *543* (7644), 270–274.
- (23) Mi, W. Y.; Guan, H. P.; Lyu, J.; Zhao, D.; Xi, Y. X.; Jiang, S. M.; Andrews, F. H.; Wang, X. L.; Gagea, M.; Wen, H.; Tora, L.; Dent, S. Y. R.; Kutateladze, T. G.; Li, W.; Li, H. T.; Shi, X. B. YEATS2 links histone acetylation to tumorigenesis of non-small cell lung cancer. *Nat. Commun.* **2017**, *8*, 1088.
- (24) Hsu, C. C.; Shi, J. J.; Yuan, C.; Zhao, D.; Jiang, S. M.; Lyu, J.; Wang, X. L.; Li, H. T.; Wen, H.; Li, W.; Shi, X. B. Recognition of histone acetylation by the GAS41 YEATS domain promotes H2A.Z deposition in non-small cell lung cancer. *Genes Dev.* **2018**, *32* (1), 58–69.
- (25) Li, X.; Li, X. M.; Jiang, Y. X.; Liu, Z.; Cui, Y. W.; Fung, K. Y.; van der Beelen, S. H. E.; Tian, G. F.; Wan, L. L.; Shi, X. B.; Allis, C. D.; Li, H. T.; Li, Y. Y.; Li, X. D. Structure-guided development of YEATS domain inhibitors by targeting pi-pi-pi stacking. *Nat. Chem. Biol.* **2018**, *14* (12), 1140–1149.
- (26) Moustakim, M.; Christott, T.; Monteiro, O. P.; Bennett, J.; Giroud, C.; Ward, J.; Rogers, C. M.; Smith, P.; Panagakou, I.; Diaz-Saez, L.; Felce, S. L.; Gamble, V.; Gileadi, C.; Halidi, N.; Heidenreich, D.; Chaikuad, A.; Knapp, S.; Huber, K. V. M.; Farnie, G.; Heer, J.; Manevski, N.; Poda, G.; Al-awar, R.; Dixon, D. J.; Brennan, P. E.; Fedorov, O. Discovery of an MLLT1/3 YEATS Domain Chemical Probe. *Angew. Chem., Int. Ed.* **2018**, *57* (50), 16302–16307.
- (27) Christott, T.; Bennett, J.; Coxon, C.; Monteiro, O.; Giroud, C.; Beke, V.; Felce, S. L.; Gamble, V.; Gileadi, C.; Poda, G.; Al-awar, R.; Farnie, G.; Fedorov, O. Discovery of a Selective Inhibitor for the YEATS Domains of ENL/AF9. *Slas Discov* **2019**, *24* (2), 133–141.
- (28) Heidenreich, D.; Moustakim, M.; Schmidt, J.; Merk, D.; Brennan, P. E.; Fedorov, O.; Chaikuad, A.; Knapp, S. Structure-Based Approach toward Identification of Inhibitory Fragments for Eleven-Nineteen-Leukemia Protein (ENL). *J. Med. Chem.* **2018**, *61* (23), 10929–10934.
- (29) Asiaban, J. N.; Milosevich, N.; Chen, E.; Bishop, T. R.; Wang, J.; Zhang, Y.; Ackerman, C. J.; Hampton, E. N.; Young, T. S.; Hull, M. V.; Cravatt, B. F.; Erb, M. A. Cell-based ligand discovery for the ENL YEATS domain. *ACS Chem. Biol.* **2020**, *15* (4), 895–903.
- (30) Luo, Z. J.; Lin, C. Q.; Shilatfard, A. The super elongation complex (SEC) family in transcriptional control. *Nat. Rev. Mol. Cell Biol.* **2012**, *13* (9), 543–547.
- (31) He, N. H.; Chan, C. K.; Sobhian, B.; Chou, S.; Xue, Y. H.; Liu, M.; Alber, T.; Benkirane, M.; Zhou, Q. Human Polymerase-Associated Factor complex (PAF) connects the Super Elongation Complex (SEC) to RNA polymerase II on chromatin. *Proc. Natl. Acad. Sci. U. S. A.* **2011**, *108* (36), E636–E645.
- (32) Niphakis, M. J.; Cravatt, B. F. Enzyme Inhibitor Discovery by Activity-Based Protein Profiling. *Annu. Rev. Biochem.* **2014**, *83* (83), 341–377.

- (33) Li, X.; Kapoor, T. M. Approach to Profile Proteins That Recognize Post-Translationally Modified Histone "Tails". *J. Am. Chem. Soc.* **2010**, *132* (8), 2504–2505.
- (34) Li, X.; Wu, Y.; Tian, G.; Jiang, Y.; Liu, Z.; Meng, X.; Bao, X.; Feng, L.; Sun, H.; Deng, H.; Li, X. D. Chemical Proteomic Profiling of Bromodomains Enables the Wide-Spectrum Evaluation of Bromodomain Inhibitors in Living Cells. *J. Am. Chem. Soc.* **2019**, *141* (29), 11497–11505.
- (35) Yang, T.; Liu, Z.; Li, X. D. Developing diazirine-based chemical probes to identify histone modification 'readers' and 'erasers'. *Chem. Sci.* **2015**, *6* (2), 1011–1017.
- (36) Liu, Z.; Yang, T.; Li, X.; Peng, T.; Hang, H. C.; Li, X. D. Integrative chemical biology approaches to examine 'erasers' for protein lysine fatty-acylation. *Angew. Chem., Int. Ed.* **2015**, *54* (4), 1149–1152.
- (37) Pidgeon, C.; Ong, S.; Liu, H.; Qiu, X.; Pidgeon, M.; Dantzig, A. H.; Munroe, J.; Hornback, W. J.; Kasher, J. S. IAM Chromatography: An in Vitro Screen for Predicting Drug Membrane Permeability. *J. Med. Chem.* **1995**, *38* (4), 590–594.
- (38) Kansy, M.; Senner, F.; Gubernator, K. Physicochemical high throughput screening: parallel artificial membrane permeation assay in the description of passive absorption processes. *J. Med. Chem.* **1998**, *41* (7), 1007–1010.
- (39) Zhu, C.; Jiang, L.; Chen, T.-M.; Hwang, K.-K. A comparative study of artificial membrane permeability assay for high throughput profiling of drug absorption potential. *Eur. J. Med. Chem.* **2002**, *37* (5), 399–407.
- (40) Jafari, R.; Almqvist, H.; Axelsson, H.; Ignatushchenko, M.; Lundbäck, T.; Nordlund, P.; Molina, D. M. The cellular thermal shift assay for evaluating drug target interactions in cells. *Nat. Protoc.* **2014**, *9* (9), 2100–2122.
- (41) Martinez Molina, D.; Nordlund, P. The cellular thermal shift assay: a novel biophysical assay for in situ drug target engagement and mechanistic biomarker studies. *Annu. Rev. Pharmacol. Toxicol.* **2016**, *56*, 141–161.
- (42) Philpott, M.; Rogers, C. M.; Yapp, C.; Wells, C.; Lambert, J. P.; Strain-Damerell, C.; Burgess-Brown, N. A.; Gingras, A. C.; Knapp, S.; Muller, S. Assessing cellular efficacy of bromodomain inhibitors using fluorescence recovery after photobleaching. *Epigenet. Chromatin.* **2014**, *7*, 14.
- (43) Li, Y. Y.; Wen, H.; Xi, Y. X.; Tanaka, K.; Wang, H. B.; Peng, D. N.; Ren, Y. F.; Jin, Q. H.; Dent, S. Y. R.; Li, W.; Li, H. T.; Shi, X. B. AF9 YEATS Domain Links Histone Acetylation to DOT1L-Mediated H3K79 Methylation. *Cell* **2014**, *159* (3), 558–571.
- (44) Arrowsmith, C. H.; Bountra, C.; Fish, P. V.; Lee, K.; Schapira, M. Epigenetic protein families: a new frontier for drug discovery. *Nat. Rev. Drug Discovery* **2012**, *11* (5), 384–400.
- (45) Greschik, H.; Schule, R.; Gunther, T. Selective targeting of epigenetic reader domains. *Expert Opin. Drug Discovery* **2017**, *12* (5), 449–463.